 doi:10.20944/preprints202012.0412.v1

Type of the Paper (Article, Review, Communication, etc.)

Synthesis of hydronium-potassium jarosite; Effect of pH and aging time on their structural, morphological and electrical properties

Elías Hernández-Lazcano[1], E. Cerecedo-Sáenz[1], J. Hernández-Ávila[1], Norman Toro[2,3] ,T. V. K. Karthik[4], D. Mendoza-Anaya[5], M. E. Fernández-García[5], V. Rodríguez-Lugo[1,*], and E. Salinas-Rodríguez[1,*]

[1] Academic Area of Earth Sciences and Materials, Institute of Basic Sciences and Engineering, Autonomous University of Hidalgo State, Highway Pachuca - Tulancingo km. 4.5, C.P. 42184, Hidalgo, Mexico; elias.dezlaz@gmail.com (E. H-L), mardenjazz@yahoo.com.mx (E. C-S), herjuan@uaeh.edu.mx (J. H-A)

[2] Faculty of Engineering and Architecture, Universidad Arturo Prat, Almirante José Latorre 2901, Antofagasta 1244260, Chile

[3] Department of Metallurgy and Mining Engineering, Universidad Católica del Norte, Antofagasta 1270709, Chile; ntoro@unc.cl (N. T.)

[4] Higher School of Tepeji - Autonomous University of Hidalgo State. Noxtongo, 42855, Tepeji del Río de Ocampo, Hidalgo. México; krishnakarthik.tv@gmail.com (T.V.K. K)

[5] National Institute of Nuclear Research. Highway Mexico - Toluca S/N, La Marquesa, 52750, Ocoyoacan, Mexico; demetrio.mendoza@inin.gob.mx (D. M-A), maria.fernandez@inin.gob.mx (M.E. F-G)

* Correspondence: salinasr@uaeh.edu.mx, Tel.: +52-7712-074-171 (E. S.-R.) & ventura.rl65@gmail.com, Tel.: +52-2225-695-166 (V. R.-L.)

Abstract: Structural and morphological properties of the hydronium-potassium jarosite microstructures were investigated in this work, and their electrical properties were evaluated. All microstructures were synthesized at a reasonable temperature of 343 K with a reduced reaction time of 3 hours. Increase in the pH from 0.8 to 2.1 decreased the particle sized from 3 μm to 200 nm and increasing the aging time from 0, 3 to 7 days resulted in semispherical, spherical and euhedreal jarosite structures, respectively. A Rietveld analysis also was done, finding that increasing pH, the amount of hydronium substitution by potassium in the cationic site also increases, having a 77.72 % of hydronium jarosite (JH) plus 22.29 % potassium jarosite (JK) at pH 0.8; 82.44 % (JH) and 17.56 % (JK) at pH 1.1, and 89.98 % (JH) plus 10.02 % (JK) at pH 2.1. The results obtained in this work show that the obtained hydronium potassium jarosite microstructures with reduced particle size and euhedreal morphology can be used as anode materials for improving the life time of lithium ion batteries, due that during the analysis of the voltage obtained using electrodes made with this particles and graphite, this ranged from 0.89 to 1.36 V.

Keywords: Hydronium jarosite; potassium jarosite; micro particles; pH; aging time; energy storage; euhedral morphology

1. Introduction

Jarosite, and echo-rich mineral pertains to trigonal crystal system with rhombohedral structure and can be acquired from sites highly acidic surroundings like in the Spanish southeast, where jarosite was found for the first time in the Jaroso Ravine in the Almagrera Sierra from where its name came [1]. Jarosite type-compounds have been of great interest mainly for mineralogists and metallurgists devoted to extractive metallurgy, because the jarosite contain valuable metals such as silver, gold, etc., in their crystalline structure which can be recovered by alkaline decomposition processes [2-5]. During the elimination of iron in the leaching process, where the residues had to be filtered and discarded jarosite [6], was predominantly used where the particle size and morphology

Preprints (www.preprints.org) | NOT PEER-REVIEWED | Posted: 16 December 2020 doi:10.20944/preprints202012.0412.v1

plays a crucial role. Large particle sizes were always preferred to improve filtering process [7]. Other important applications of nano or micro structured potassium jarosite are spin chirality on a 2D geometrically frustrated lattice, geochemical indicators due to their unique structural and magnetic properties [8, 9].

On the other hand, jarosite is a mineral that is found all over the planet and been detected in Mars [10]. It can be found in acidic sulfate soils, oxidized zones of sulfur mineral deposits, hydrometallurgical systems, bioleaching systems and in environments contaminated by acid mine drainage [11]. Also, it has been proven that jarosite type-compounds are better absorbents of dangerous wastes in comparison with other minerals for the elimination of toxic metals due to the presence of these toxic elements in the crystalline structure of the jarosite type-compounds [12-14].

Mineralogically, jarosite belongs to the isostructural family of minerals "Jarosite - Alunite", which general formula is: $AB_3(SO_4)_2(OH)_6$, where A can be, H_3O, Na, Rb, Ag, K, NH_4, ½Pb or ½Hg, and B can be Al (III), Cu (II) or Fe (III). Thus, potassium jarosite is a hydrated mineral that contains alkalis and ferric iron with chemical formula like: H_3O-$KFe_3(SO_4)_2(OH)_6$ [15-17]. For decades, the properties of this mineral as well as the conditions of synthesis and decomposition have been studied widely, principally for employing in the zinc industry process to precipitate non - desired iron and other elements and to facilitate the filtering process. But also, recently, studies on this mineral have been carried out as they can also provide information on the geochronology and climate of the area in which they are found [12, 18].

Wide range of researchers carried out experiments to synthesize jarosite under laboratory conditions (synthetic jarosite) where the principal characteristics employed during the synthesis were high synthesis temperatures (> 363 K) and time (> 24 h) [2-5]. For example, alkaline decomposition of the jarosite type-compounds obtained with the synthesis temperatures between 366 and 371 K and time ~ 24 h was executed, where the obtained particles sized where from 20 to 80 μm in diameter [13, 19-22]. Additionally, synthesis of jarosite particles with very small diameters, close to nanometric values, were reported but with the disadvantage that it is necessary the presence of other agents such as potassium fluoride, δ-MnO_2 nanosheets and other variables in addition to the traditional wet chemical synthesis method [14, 23, 24]. Until now, different synthesis methods have been developed with different synthesis parameters for obtaining jarosite structures, but wet chemical synthesis method is the most simple, precise and cost-effective method for obtaining size and morphology controlled jarosite micro structures [13].

Traditionally, jarosites have been synthesized to eliminate Fe from hydrometallurgical solution from electrolytic zinc recovery, and other applications; however recent investigation have paid attention to the use of this type of compounds as anodes and/or cathodes in lithium ion batteries. In the case of its use as cathode, it was developed a scalable method to prepare a two-dimensional material composed by and hybrid material of potassium jarosite/rGO, via a solution - phase oxidation process at elevated temperature, where the graphene oxide sheets acted as a surface where occurred a direct growth of mono crystals of potassium jarosite [24]. Therefore, the $KFe_3(SO_4)_2(OH)_6$/rGO hybrid material so synthesized has demonstrated a great potential for application as a high-performance cathode material in new-generation lithium-ion rechargeable batteries. In this way, these kind of materials have attracted the attention of researchers for their application as cathodes in lithium ion batteries, particularly potassium jarosite ($KFe_3(SO_4)_2(OH)_6$ and sodium jarosite ($NaFe_3(SO_4)_2(OH)_6$, where the unique topotactic reversible reaction could be the explanation of the electrochemical process of jarosites type hydrosulfates, which could indicate its energy storage capability [6]. In the same way, Ding et al. [25] used a template-assisted redox method to synthesize nanosheets of potassium jarosite that delivered a large specific capacity of 117 mA h g^{-1} at 0.2C and about 80 mA h g^{-1} at 10C after 50 cycles, showing excellent rate capability and capacity retention.

Other researchers have pointed that the crystalline structure of these king of compounds, the alkaline elements involves such as K and Na, and the morphology play an important role for the intercalate and deintercalate of small ions like Li^+ between the layers. In theory, there are three lithium ions that can be intercalated and deintercalted in per formula of $KFe_3(SO_4)_2(OH)_6$ crystal

Preprints (www.preprints.org) | NOT PEER-REVIEWED | Posted: 16 December 2020 doi:10.20944/preprints202012.0412.v1

structure in the potential range of 1.5 - 4 V vs. Li/Li^{+}, via reduction/oxidation between Fe^{3+} and Fe^{2+}, which corresponds to a theoretical capacity of 166 mA h g^{-1}, which makes it a promising cathode material for LIBs [16, 26-28].

All the above studies and others, related to the jarosite type-compounds have managed to find interesting advances, not only in the innovation of obtaining these materials, which by modifying parameters and synthesis methods have found appropriate morphologies and particle sizes to be able to evaluate new properties that place them as a material with possible applications in new fields such as that of energy storage. Currently the field of portable electronics continues to be monopolized by first generation $LiCoO_2$ layered cathodes in Lithium-Ion Batteries (LIBs) and recent research has turned in favor of removing Co due to its toxicity and method of obtaining. For this reason, they are looking for new materials that are low cost with great capacity to behave either as anode or cathode [29-31].

Therefore, this work demonstrates the improvements such as low operation temperature (343 K), low synthesis time (3 h), changes in pH and aging time applied to the traditional method of synthesis for the jarosite type-compounds to obtain a new modified method making the synthesis both economic and environmental friendly. Changes in pH (0.8, 1.2 and 2.1) and the aging time (0, 2 and 7 days) after the synthesis, have contributed significantly in the reduction of the particle size and morphologies spherical and euhedreal. Some authors have pointed that the high crystalline structure of jarosite type compound, its particle size and morphology, have great impact in the cycle-life and experimental achievable capacity for the galvanostatic charge-discharge in the LIBs [32]. Finally, the so obtained synthetic jarosite structures could be utilized as a novel material in Li ion batteries according with the results obtained in the Daniell Cell for the electrodes made of jarosite and graphite.

2. Materials and Methods

2.1. Synthesis of hydronium-potassium jarosite

Synthesis of potassium jarosite employed in this work was similar to the method reported by Dutrizac and Kaiman [33], and Salinas *et al.* [19] with considerable modifications. And were prepared modifying the method used as well as all chemicals, Iron (III) sulfate, $Fe_2(SO_4)_3$ and potassium sulfate, K_2SO_4, as source of potassium jarosite; sodium hydroxide, NaOH and sulfuric acid, H_2SO_4, were utilized for adjusting pH in this work and were purchased from Sigma Aldrich with high purity (> 99 %). In the present work, 0.15 M of $Fe_2(SO_4)_3$ and K_2SO_4, aqueous solutions were separately prepared. In a 0.5 L three-neck flask containing the mixture of $Fe_2(SO_4)_3$ and K_2SO_4 in 0.3L deionized water equipped with pH measurements system, whose temperature was maintained at 343 K. Fig. 1 shows the experimental setup for obtaining the jarosite powders.

Preprints (www.preprints.org) | NOT PEER-REVIEWED | Posted: 16 December 2020 doi:10.20944/preprints202012.0412.v1

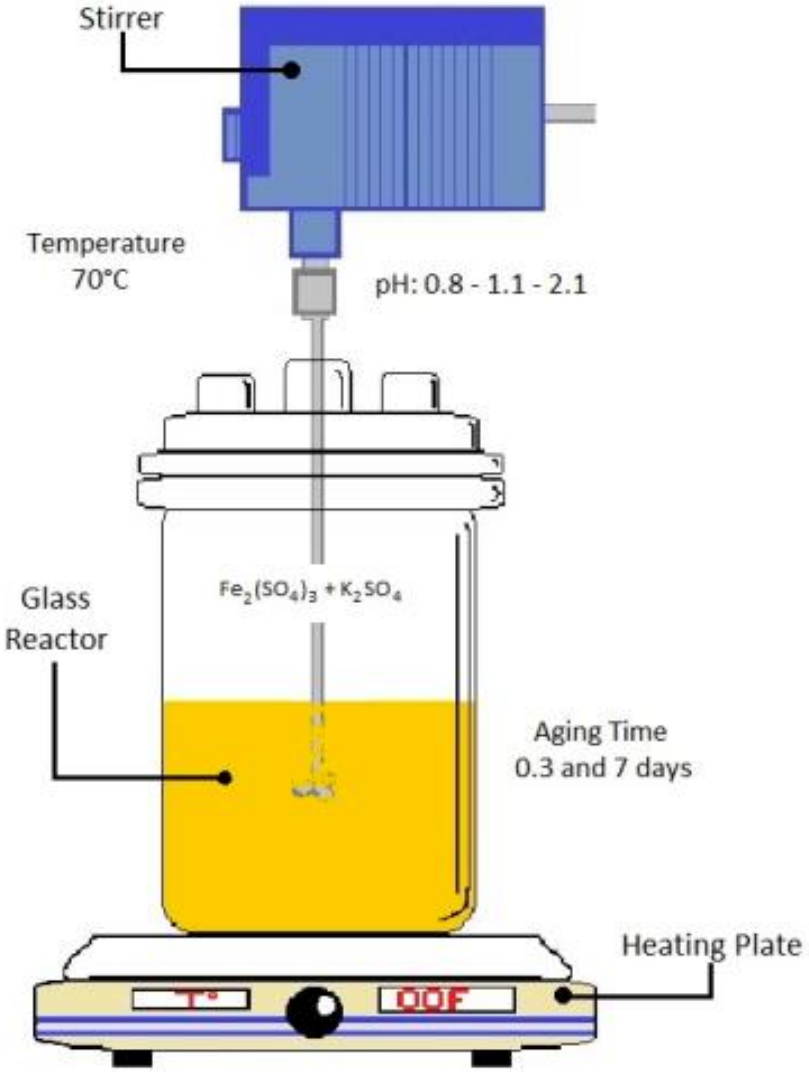

Figure 1. Experimental apparatus mounted to synthesize the potassium jarosite

The above mixed solution has a pH 1.1 and it was left for 3 h with a stirring rate ~ 200 s^{-1}, which results in brown precipitates. The procedure was replicated for pH 0.8 and 2.1 samples just by adding H_2SO_4 and NaOH, respectively, drop wise through the left neck of the flask by monitoring the pH with a potentiometer placed in the right neck of the flask. The reaction time ~ 3 h, synthesis temperature ~ 343 K and stirring rate 200 s^{-1} were kept constant for all the samples. Finally, precipitates in each case were collected separately, filtered and dried at room temperature. Additionally, two more samples with pH 2.1 were synthesized with an additional aging time of 3 and 7 days before the filtration of precipitates. All the samples obtained are shown in table 1.

Table 1. List of samples with their synthesis conditions obtained in this work.

Sample name	pH	Aging time
Jar-0.8-0	0.8	0
Jar-1.1-0	1.1	0
Jar-2.1-0	2.1	0
Jar-2.1-3	2.1	3
Jar-2.1-7	2.1	7

Preprints (www.preprints.org) | NOT PEER-REVIEWED | Posted: 16 December 2020 doi:10.20944/preprints202012.0412.v1

2.2. Material Characterization

All the obtained jarosite powders synthesized were characterized by Low Vacuum Scanning Electron Microscopy (LV-SEM) in a JEOL JSM5900-LV machine equipped with an Oxford EDS and operated at 20 kV to observe surface morphology, chemical composition and the effect of pH and sintering temperature on the particle size. The X-ray diffraction analysis was carried out by the powder technique in a Bruker D8 Discover diffractometer, with a CuKα = 1.5406 Å radiation source, operating at 40 kV and 40 mA. Diffraction patterns were collected in a 2θ range from 10° to 70° with an increment step size of 0.03°to identify the phase compound and the crystalline structure of jarosite. Finally, the X ray diffraction patters were subjected to a Rietveld analysis using a Topas[2] software; R[3e] factor and χ^2 were parameters used to indicate the accuracy of this refinement of XRD patters.

2.3. Preparation of electrodes and evaluation of electrical conductivity

To evaluate the electrical properties of the powders of hydronium-potassium jarosite, electrodes of a mixture of jarosite and graphite were prepared. The procedure to elaborate the electrodes was the following; 0.1 g of graphite was weighed for each electrode, and from each jarosite sample 0.1 and 0.5 g were weighed respectively to obtain two electrodes from each sample. Then 15 to 20 of silicone oil were added with a syringe to form the paste that was subsequently deposited on a piece of transparent plastic acetate that served as a mere support for the paste, as is shown in Figure 2.

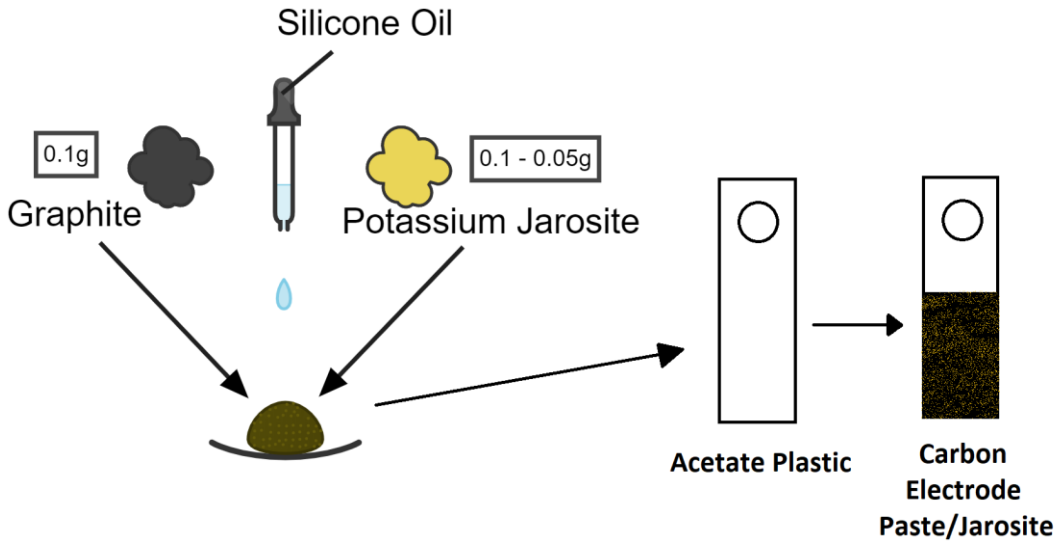

Figure 2. Elaboration of the electrodes for the evaluation of the electrical properties of jarosite

To carry out the electrical tests of the hydronium-potassium jarosite samples, an arrangement like the one shown in Fig. 3, the tests were carried out with calcium chloride ($CaCl_2$) as electrolyte in order to evaluate the behavior of the electrodes.

Preprints (www.preprints.org) | NOT PEER-REVIEWED | Posted: 16 December 2020 doi:10.20944/preprints202012.0412.v1

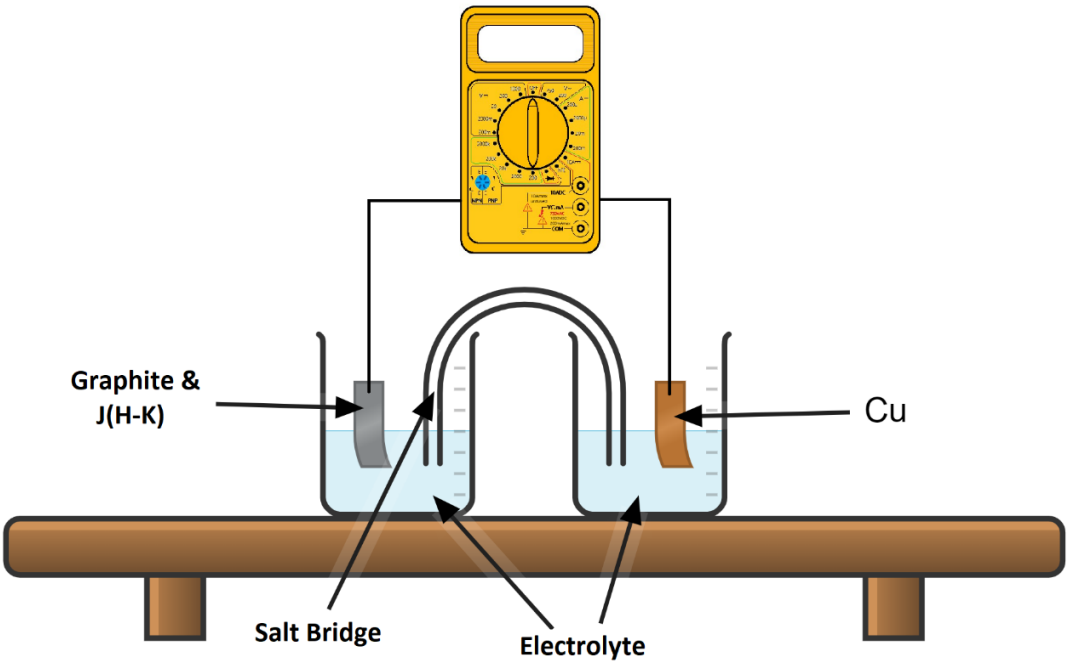

Figure 3. Experimental arrangement for electrical tests (Daniell´s cell)

For the electrical tests, a supersaturated solution (60 ml) of calcium chloride ($CaCl_2$) in injectable water was prepared to be used as electrolyte, a Cu coin was used as cathode, and the different electrodes prepared with paste of carbon + Jarosite synthesized at different pH´s.

3. Results and discussion

3.1. XRD Analysis

The X-ray diffraction patterns of synthesized potassium jarosite powders obtained for all samples are shown in Fig. 4. A glance on patterns shows the formation of synthetic potassium jarosite (H_3O-K)$Fe_3(SO_4)_2(OH)_6$) with preferential orientation in (113) plane. It is evident from Fig. 4 that all the powders exhibit the rhombohedral structure of potassium jarosite matching with International Centre for Diffraction Data Powder Diffraction Files (ICDD PDF 22-0827). All samples with different pH values and aging times synthesized showed a well-defined crystallinity, and no other peaks related to different jarosite forms, or products related to precursor residues can be identified; therefore, a solid solution of hydronium - potassium jarosite powders were synthesized.

Preprints (www.preprints.org) | NOT PEER-REVIEWED | Posted: 16 December 2020 doi:10.20944/preprints202012.0412.v1

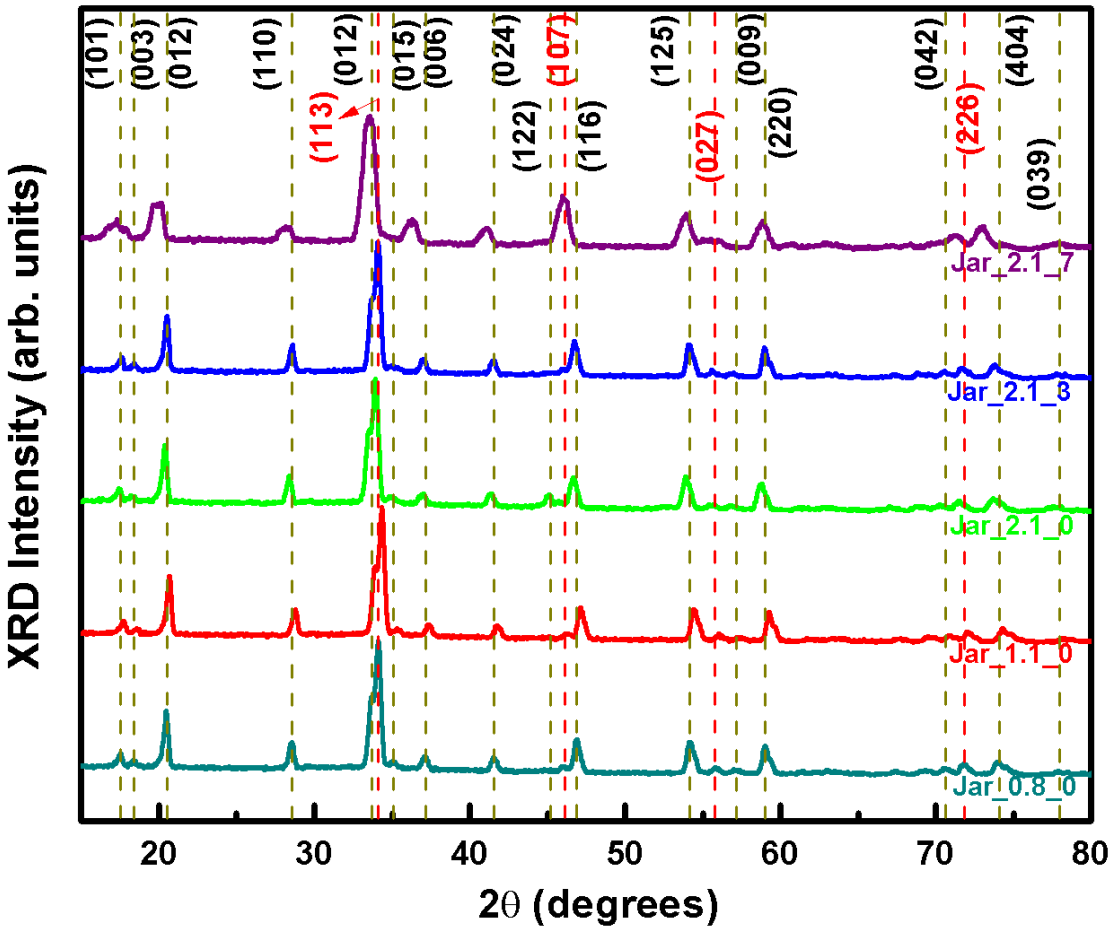

Figure 4. XRD spectrums for samples obtained at different pH values of 0.8 (Jar_0.8_0); 1.1 (Jar_1.1_0) and 2.1 (Jar_2.1_0), and aging time of 0 days (Jar_2.1_0), 3 days (Jar_2.1_3) and 7 days (Jar_2.1_7)

In comparing all the XRD patterns, irrespective of aging time, all the diffraction peaks were narrow and well separated with increase in pH. It confirms that samples improved their crystallinity and increased crystallite size (Table. 2) due to the reduction in strain and defect density of the crystal. Whereas an increase in the aging time has made the diffraction patterns broader and connected. A keen observation of Fig. 4, it is evident that with the increase in the aging time, intensities of all the planes decreases and planes like (003), (015), (006), (027) and (009) try to vanish which is corroborated to the increase in the chemical reactivity between the species involved resulting in decomposition of the jarosite structures in the presence of the ionized residues after the precipitation with increased aging time. Increase in the pH of the samples there is neither difference in the plane intensities nor in the number of planes.

Presence of precipitates during the aging makes the structures to react with the released ions like H_3O^+, K^+, Fe^{3+}, and OH^-, which restricts the growth in desired planes or vanishes some planes. We believe that the presence of adequate OH- ions for the pH value 2.1 resulted in lower crystallite size and deviated lattice parameters.

On the other hand, both increase in pH and aging time there is shift in the principle (113) plane for all jarosite structures, which is replotted and shown in Fig. 5. In order to ascertain the effect of pH and aging time the line broadening analysis of (113) peak using Debye Scherrer equation was employed and found the crystallite size and lattice parameters for all samples and tabulated in Table 2.

Preprints (www.preprints.org) | NOT PEER-REVIEWED | Posted: 16 December 2020 doi:10.20944/preprints202012.0412.v1

Table 2. Crystallite size and lattice parameters of jarosite powders for different aging times and pH values

Sample name	Average crystallite size (nm)	a (nm)	c (nm)
Jar-0.8-0	14.5	7.316	17.15
Jar-1.1-0	12.2	7.2995	17.12
Jar-2.1-0	9.48	7.2748	17.10
Jar-2.1-3	10.67	7.2837	17.12
Jar-2.1-7	7.83	7.2684	17.07
ICDDPDF 22-0827	--	7.29	17.13

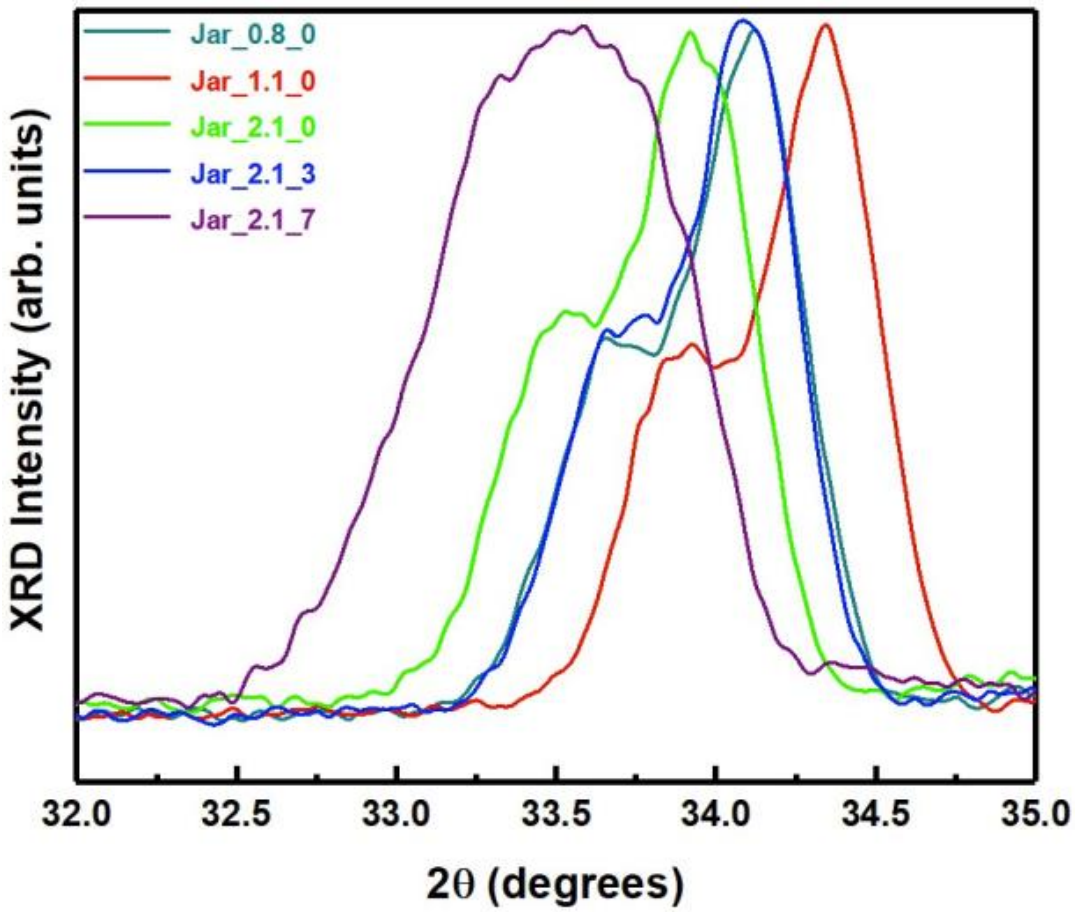

Figure 5. XRD (113) peak shift for all potassium jarosite structures

By comparing Table 2 and Fig. 5 it is evident that the decrease in pH from 1.1 to 0.8 increased the crystal size and lattice parameters showing a right shift due to the substitution of hydronium by the potassium cation occurred in the jarosite structures. Whereas increase in pH from 1.1 to 2.1 reduced the crystal size and lattice parameters noting a left shift in the preferential orientation occurred due to the above mentioned. Additionally, increase in the aging time from 0 to 3 and 7 days a peak broadening, shift in the (113) peak and vanishing of (012) plane is noticed. Powders synthesized without any modification utilizing sulfuric acid or ammonium hydroxide with pH 1.1 present the lattice parameters in consistent with the theoretical synthetic jarosite lattice parameters. Whereas the lattice parameters are largely deviated for the aged powders and slightly deviated for the powder with different pH. Crystallite size and lattice parameters decrease drastically for

Preprints (www.preprints.org) | NOT PEER-REVIEWED | Posted: 16 December 2020 doi:10.20944/preprints202012.0412.v1

powders with 7 days aging time. This is due to the decomposition of the planes of the jarosite structures and the hydronium substitution produced during the decomposition of the planes in the aged powders. This clearly evidences that the pH and aging time causes a great hydronium substitution in the jarosite structure, which results in changes of the crystal size and lattice parameters.

Because NaOH was used to control pH values, a Rietveld analysis was done (like was described in section 2.2) to determine if sodium jarosite was formed during synthesis. Table 3 shows the Rietveld results, where can be observed that only the potassium jarosite was formed with important substitution of hydronium, given so a solid solution of hydronium-potassium jarosite. In conclusion, it was found that increasing pH, the amount of hydronium substitution by potassium in the alkaline site of jarosite, also increases.

Table 3. Rietveld analysis for the synthesis of jarosite, effect of pH (0.8, 1.1 and 2.1)

Sample name	Potassium jarosite (JK) (%)	Lattice parameters		Hydronium jarosite (JH) (%)	Lattice parameters	
		a (nm)	c (nm)		a (nm)	c (nm)
Original	---	7.2900	17.1600	---	7.3238	17.005
Jar-0.8-0	22.29	7.3840	17.0320	77.71	7.3238	17.005
Jar-1.1-0	17.56	7.3105	17.2731	82.44	7.3287	17.005
Jar-2.1-0	10.02	7.2913	17.1744	89.98	7.3052	16.9700

3.2. Scanning Electron Microscopy (SEM) and Energy Dispersive Spectrometry (EDS) analysis

SEM and EDS were employed to obtain the morphological and compositional properties of the jarosite powders and subsequently interpret their association with the structural properties. Fig. 6 shows the SEM images of the potassium jarosite powders synthesized pH values 0.8 (Figs. 6a and 6b), 1.1 (Figs. 6c and 6d) and 2.1 (Figs. 6e and 6f); aged for 0 (Figs. 6e and 6f), 3 (Figs. 6g and 6h) and 7 (Figs. 6a and 6b) days. The EDS analysis of all the samples were resumed and tabulated in Table. 3.

Jarosite powders show similar agglomerates ~ 2 μm, for samples prepared with pH values 0.8 and 1.1 (refer Figs. 6a-6d). As prepared powders with pH 1.1 show a morphology a dense morphology with very broad distribution of grain size ranging from 500 nm to 3 μm (Figs. 6c-6d). Decrease of pH to 0.8 by adding sulphuric acid, size of the agglomerates and density of the particles decreased (Figs. 6a-6b) due to the relative reduction of OH^- ion concentration. In both samples with pH values 0.8 and 1.1 no specific morphology was observed, only agglomerates with random size and density were noticed. As the pH value increased to 2.1, exceptionally, an elliptical or semi-spherical morphology with particle size around 1 μm of the jarosite particles were observed (Figs. 6e, and 6f). Powders with similar pH 2.1 with increased aging time of 3 and 7 days the morphology changed drastically to spherical and euhedreal structures, respectively (Figs. 6g-6j). Particle sizes around 500 and 200 nm were obtained for powders aged for 3 and 7 days respectively. Particle size decreased with increase in aging time from 2 μm to 200 nm. The particles sizes obtained in SEM are in contrast with XRD crystallite sizes. Therefore we believe that the particles observed in SEM are constituted with smaller crystallites.

As prepared jarosite solution is acidic with pH 1.1 and as the pH of solution is increased by addition of strong base, NH_4OH, mainly K^+ and OH^- ions are liberated which makes the solution

Preprints (www.preprints.org) | NOT PEER-REVIEWED | Posted: 16 December 2020 doi:10.20944/preprints202012.0412.v1

more soluble and these OH^- ions are situated on the facets of the formed nuclei [26]. Later the growth and agglomeration are restricted by OH^- ions resulting some elliptical particles (Figs. 6e and 6f). When the precipitates are left in the supernatant for 3 days, increased H_3O starts incorporating into the structure and allowing the growth in a direction which resulted in the spherical like morphology (Figs. 6g and 6h). Furthermore, increase in the aging time to 7 days, besides incorporation of the H_3O, majority of the planes starts decomposing and forms particles with different facets resulting in euhedral potassium jarosite structures (Figs. 6i and 6j). Therefore, pH is a very important parameter to obtain the desired surface morphology. The decomposition of the planes is clear from the XRD analysis (Figs. 4 and 5) where the planes (012) and (113) reduces to only (113) confirming the decomposition of planes and subsequently resulting euhedral structures (Fig. 6j). For contemplating the liberation and incorporation of cations and anions in each sample EDS analysis was performed and the obtained results were tabulated in Table. 4.

Table 4. EDS point analysis of all the synthesized samples compared with the theoretical and synthesized values reported [33].

Element or compound	Theoretical	Synthetic	J-K_0.8_0	J-K_1.1_0	J-K_2.1_0	J-K_2.1_3	J-K_2.1_7
K	7.81	7.17	5.50	6.20	6.72	7.02	7.15
Fe	33.45	29.50	20.20	20.90	21.20	21.48	21.43
SO_4	38.36	40.70	39.84	38.95	40.14	43.44	44.70
H_3O + OH*	20.38	22.63	34.56	33.95	31.94	28.06	26.72

** Calculated by difference and considering the incorporation of H_3O into jarosite structure*

In Table 4 we compare the obtained elemental composition values with the theoretical and synthetic jarosite composition values reported by the traditional synthesis method employed firstly by Dutrizac and Kaiman [33]. According to the obtained EDS results, it can be observed that the values of K and Fe closer to the values reported in the traditional synthesis method with increase in pH from 0.8 to 2.1 which we believe is due to the utilization of very less molar concentration (0.15 M) compared to reported work. Whereas, the contents of SO_4 and (H_3O + OH) were relatively higher which is conventional because as the quantity of anions liberated increases, the solution pH also increases, pH utilized in the theoretical and synthetic jarosite was 1.2. Therefore, by comparing XRD, SEM and EDS analysis it can be concluded that the aging time makes the jarosite to form euhedreal structures and increased pH makes the size of the particle more micrometric. The results obtained in this work are the preliminary work, where in future detailed analysis of aging time and pH is studied to obtain the nanometric jarosite structures.

Preprints (www.preprints.org) | NOT PEER-REVIEWED | Posted: 16 December 2020 doi:10.20944/preprints202012.0412.v1

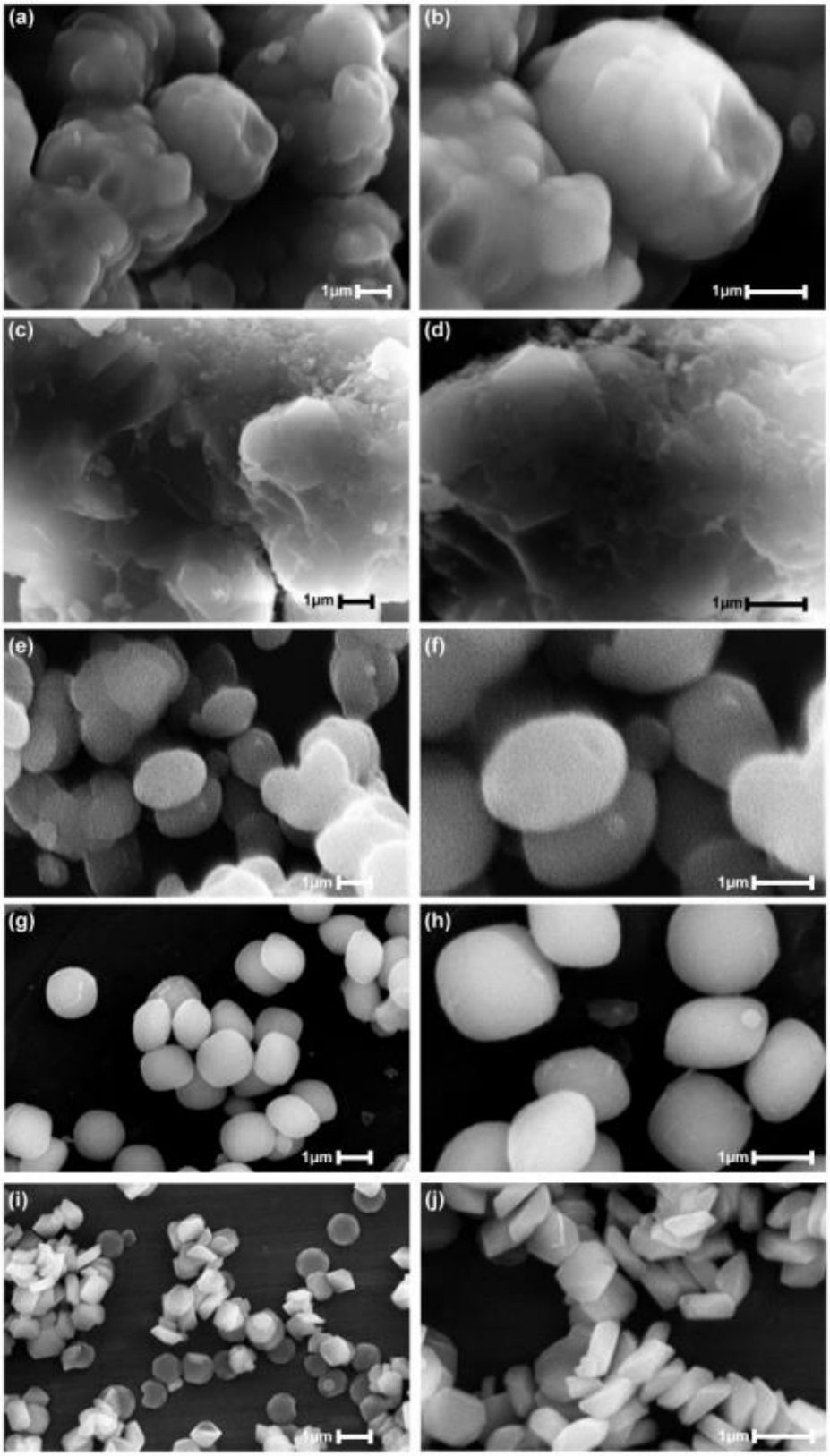

Figure 6. SEM image of potassium jarosite particles synthesized at different conditions: (a, b) pH 0.8, (c, d) pH 1.1, (e, f) pH 2.1 with no aging time, (g, h) pH 2.1 with 3 days aging time and (i, j) pH 2.1with 7 days aging time. Left and right column images are with magnifications 10,000x and 20,000x, respectively.

Preprints (www.preprints.org) | NOT PEER-REVIEWED | Posted: 16 December 2020 doi:10.20944/preprints202012.0412.v1

3.3. Electrical analysis

According the obtained results during electrical tests, it can be seen in Table 5 that the electrochemical reaction executed by the electrodes prepared with hydronium-potassium jarosite and graphite gave good results. Table 5 shows that the best results found were for the jarosite synthesized at pH 2.1 with 3 and 7 days of aging, where morphology is spherical and euhedreal, respectively.

Table 5. Results obtained during electrical test done on electrodes prepared with jarosite and graphite, using calcium chloride as electrolyte

Electrode	Registry (V)	Reverse (V)
Cu coin	0.52	-
Graphite_0.1g (G1)	0.89	-0.90
G1/J(HK)_0.8_0 (0.1g)	0.90	-0.95
G1/J(HK)_0.8_0 (0.05g)	0.90	-1.01
G1/J(HK)_1.1_0 (0.1g)	0.96	-0.99
G1/J(HK_1.1_0 (0.05g)	0.89	-0.90
G1/J(HK)_2.1_0 (0.1g)	0.94	-0.95
G1/J(HK)_2.1_0 (0.05g)	0.90	-0.96
G1/J(HK)_2.1_3 (0.1g)	1.00	-1.00
G1/J(HK)_2.1_3 (0.05g)	1.35	-1.42
G1/J(HK)_2.1_7 (0.1g)	1.36	-0.98
G1/J(HK)_2.1_7 (0.05g)	1.00	-1.05

According to these preliminary results, it can be seen that the jarosite synthesized at pH 2.1 and with a resting time of 3 and 7 days, shows the best results, obtaining an average potential of 1.35 V, which is close to the potential generated by a standard battery that is 1.5 V and a little above the voltage generated by the rechargeable battery that is 1.2 V.

These results also indicate that particle size and morphology play an important role, since these materials have average particle sizes ranging from 1 to 0.2 microns, and spherical and euhedreal morphologies (Figs. 6g-h and 6i-h), which coincide with some researchers who pointed that the particle size and morphology of crystalline jarosite play an important role in the ability of these compounds to serve as cathode in LIB´s [6,32].

4. Conclusions

Wet chemical synthesis of potassium jarosite powders was successfully performed and synthesis performed at reduced synthesis temperature at 70 °C and for only 3 h of reaction time. The results obtained in this work directs that the morphological and micro-structural properties of the hydronium-potassium jarosite obtained have a strong dependency on synthesis parameters, mainly to the pH of the solution and the aging time. For samples with pH 0.8 and 1.1, dense agglomerates around 3-2 μm were formed, with an increase of pH to 2.1, elliptical or non-spherical particles ~1 μm were observed. Increasing in aging time from 0 to 3 days resulted in pure spherical particles ~500 nm. Furthermore, increase in aging time to 7 days, euhedreal structures ~ 200 nm were obtained. Increase in pH and aging time has decreased the particle size and changed the morphology from elliptical to spherical and euhedreal structures. XRD patterns confirms that all samples synthesized with the new method, are concordant with the ICDD PDF 20827 of the $(H_3O\text{-}K)\ Fe_3(SO_4)_2(OH)_6$ with a preferential orientation (113) plane with good crystalline structure. No other peaks related to different jarosite forms are identified. Increase in aging time confirms the

Preprints (www.preprints.org) | NOT PEER-REVIEWED | Posted: 16 December 2020 doi:10.20944/preprints202012.0412.v1

decomposition of the planes, which is in good agreement with the SEM results. Increase in the pH released ions like K^+, Fe^{3+}, and OH^-, which restricts the growth in desired planes or vanishes some others, which is also evidenced through the EDS analysis. Compared to the theoretical and synthetic jarosite powders, the powders obtained in this work are relatively a solid solution of hydronium-potassium jarosite with less particle size and the synthesis conditions utilized make the process easier and cost effective. These kind hydronium-potassium jarosite powders show by the Rietveld analysis that increasing pH to 2.1, hydronium substitution by potassium in alkaline site of the jarosite structure, also increases. Finally, according the results obtained in the electrical tests done is this work, this kind of powder can be utilized as new cathode material in Li ion battery applications, because in the electrical tests executed the nominal voltage obtained (1.3 V) is close to the standard battery (1.5 V) and a little above that of the rechargeable battery (1.2 V). Finally, table 6 show the results obtained in this work in comparison with other done by some researches along the time, according the morphology, particle size and electrical properties of these kind of solid solutions.

Table 6. Comparative description of some works done along time, related with the synthesis of jarosite type compounds and their characteristics

Author	Jarosite	Synthesis conditions	Results
J.B. Brown, 1970 [34]	K	298 K, 1 atm, pH 0.9-2.22, time 6 weeks-6 months	Potassium jarosite
W. Kunda et al., 1979 [35]	NH_3-Na	453-463 K, 350 KPa, 0.75 h retention time	Agglomerates > 10 µm
F. Patiño et al., 1993 [36]	Ag-Pb	370 K, 24 h, 500 s^{-1}	Rhombohedral crystals, semispherical particles 80-100 µm
J.E. Dutrizac et al., 1997 [37]	K	371 K, 24 h, 500 s^{-1}, pH 1.6	Agglomerates
M Cruells et al., 2000 [38]	Ag	370 K, 24 h, jarosite seeds	Semispherical particles > 30µm
C. Drouet et al., 2003 [16]	K-Na-H_3O	368 K, 4 h, dehydrated overnight at 383 K	ICDD PDF 220827
J.L. Cadena et al., 2006 [39]	K	373 K, 24 h, 500 s^{-1}, pH 1.5, dried at 283 K for 24 h	Cauliflower particles > 30µm
A. Roca et al., 2007 [40]	NH_4-H_3O-Ag	367 K, 24 h, pH 1.8, using seeds to increase particle size	Spherical particles of 37 - 44 µm
L. Gunneriusson et al., 2009 [23]	K-F	343 K, 48 h, dried 3 days at room temperature, pH 1.6	Agglomerates of particles ~ 1 µm
E. Salinas et al., 2012 [19]	Ag-Rb	367.5 K, 24 h, pH 1.2	Particles 20-30 µm
W. Xu et al., 2016 [24]	K-based GO	Graphene oxide layers, 353 K, 12 h, stirred for 10 h at 298 K	Bulks of JK > 10µm, with nanoplates width ~ 800 nm and thickness ~ 100 nm, reversible capacity of 70.7 mAh g^{-1}
N. Wu et al., 2019 [29]	K-rGO nanosheets	Dissolution of KNO_3-$FeSO_4 7H_2O$-GO.	Particle size over 4 µm. 545 mAh g^{-1} at the end of 1000 cycles at 500 mAh

		383 K (autoclave) during 12 h.	g^{-1}
This Work	*H_3O-K*	***343 K, 3 h, pH(0.8, 1.1 and 2.1), aging time 0, 3 and 7 days.***	***Particle sizes varying from agglomerates 5 to 10 μm to individual particles from 0.2 to 1 μm. Morphologies from quasi spherical, elliptical, spherical and euhedral. With electrical properties generating from 0.89 to 1.36 V in the Daniell cell***

Author Contributions: Conceptualization, E. S-R and E. H-L; methodology, E. C-S and E. S-R; software, M.E. F-G; validation, D. M-A, V. R-L and N. T; formal analysis, E. S-R; investigation, E. H-L; data curation, J. H-A; writing—original draft preparation, E. S-R and V. R-L; writing—review and editing, T.V.K. K. and N. T; visualization, T.V.K. K; supervision, E. S-R and J. H-A; project administration, E. S-R, E. C-S, V. R-L. All authors have read and agreed to the published version of the manuscript

Funding: This research received no external funding.

Acknowledgments: Authors want to thank to thank the CONACyT of the Mexican Government for the support with the scholarship awarded to the doctorate student with CVU 781801. Authors also thank Authors also thank to the academic support program PRODEP of the Secretary of Public Education of Mexico.

Conflicts of Interest: The authors declare no conflict of interest.

References

1. C. Nuñez and A. Roca. Concentration of Iron Oxides by Flotation From Gossan Ore Tailings. *Can. Metall. Q.* **1984**, *23,* 393-397. https://doi.org/10.1179/cqm.1984.23.4.393
2. F. Patiño, E. Salinas, M. Cruells and A. Roca. Alkaline decomposition-cyanidation kinetics of argentian natrojarosite. *Hydrometallurgy*. **1998,** *49 (3),* 323-336. https://doi.org./10.1016/S0304-386X(98)00041-3
3. M. Cruells, A. Roca, F. Patiño, E. Salinas, I. Rivera. Cyanidation kinetics of argentian jarosite in alkaline media. *Hydrometallurgy*. **2000,** *55 (2),* 153-163. https://doi.org/10.1016/S0304-386X(99)00072-9
4. F. Patiño, M. Cruells, A. Roca, E. Salinas and M. Pérez. Kinetics of alkaline decomposition and cyanidation of argentian ammonium jarosite in lime medium. *Hydrometallurgy*, **2003,** *70 (1-3),* 153-161. https://doi.org/10.1016/S0304-386X(03)00074-4
5. F. Patiño C., E. Salinas R., J.J. Canales S., P. Ávila P., I. Rivera L., J.M. González L., M. Reyes P. Synthesis of argentian plumbojarosite and its reaction stoichiometry in NaOH and NaCN media. In: European Metallurgical Conference 2007, June 11 – 14, Düseldorf, Alemania. Processings Volume 3. (Zinc and Lead) 2007, pp. 1209 – 1220. (https://www.yumpu.com/en/document/read/3611673/volume-1-emc-european-metallurgical-conference-gdmb-)
6. Y.L. Ding, Y. Wen, C.C. Chen, P.A. Van Aken, J. Maier, and Y. Yu. Nanosheets of earth-abundant jarosite as novel anodes for high-rate and high-life lithium-ion batteries. *ACS Appl. Mater. Interfaces.* **2015,** *7(19),* 10518-10524. DOI: 10.1021/acsami.5b01992
7. K.A. Hudson-Edwards, A.M.L. Smith, W.E. Dubbin, A.J. Bennettt, P.J. Murphy and K. Wright. Comparison of the structures of natural and synthetic Pb-Cu-jarosites-type compounds. *Eur. J. Mineral.* **2008,** *20,* 241-252. DOI: 10.1127/0935-1221/2008/0020-1788.
8. E. Salinas, A. Roca, M. Cruells, F. Patiño, D.A. Córdoba. Characterization and alkaline decomposition-cyanidation kinetics of industrial ammonium jarosite in NaOH media. *Hydrometallurgy*, **2001,** *60 (3),* 237 – 246. https://doi.org/10.1016/S0304-386X(01)00149-9
9. K.A. Hudson-Edwards, A.M.L. Smith, W.E. Dubbin and K. Wright. Jarosite in acid mine drainage environments: Formation, mineralogy, stability. In: (Proceedings) 15th Annual V. M. Goldschmidt

Conference, May, Moscow, Idaho, USA, 2005, Pp. A765. (https://goldschmidt.info/2005/Abstract%20Volume/abs_vol.pdf)

10. E. Salinas, M. Reyes, F. Patiño, M. T. Méndez, I. Rivera, A. Martínez and L. Hernández. Factores que afectan el crecimiento de partículas de jarosita de amonio argentífera sintética (In spanish). *Rev. Soc. Quim. Mex*. **2002,** *46 (1),* 67-72. http://www.scielo.org.mx/pdf/rsqm/v46n1/v46n1a12.pdf
11. W. H. Farrand, T. D. Glotch, J. W. Rice Jr., J.l A. Hurowitz, G. A. Swayze. Discovery of jarosite within the Mawrth Vallis region of Mars: Implications for the geologic history of the region. *Icarus*, **2009,** *204 (2),* 478 – 488. https://doi.org/10.1016/j.icarus.2009.07.014
12. M. Kerolli-Mustafa, H. Fajković, S. Rončević & L. Ćurković. Assessment of metals risks from different depths of jarosite tailing waste of Trepça Zinc Industry, Kosovo based on BCR procedure. *J. Geochem. Explor.* **2015,** *148,* 161 – 168. http://dx.doi.org/10.1016/j.gexplo.2014.09.001
13. I. Mireles, I. A. Reyes, V.H. Flores, F. Patiño, M.U. Flores, M. Reyes, M. Acosta, R. Cruz and E. J. Gutierrez. Kinetics analysis of the decomposition of the $KFe_3(SO_4)_{2-x}(CrO_4)_xOH)_6$ jarosite solid solution in $Ca(OH)_2$ medium. *J. Braz. Chem. Soc*. **2016,** *27 (6),* 1014 - 1025. https://www.scielo.br/pdf/jbchs/v27n6/0103-5053-jbchs-27-06-1014.pdf
14. R. Zhao, Y. Li, and C. K. Chan. Synthesis of jarosite and Vanadium jarosite analogues using microwave hydrothermal reaction and evaluation of composition-dependent electrochemical properties. *J. Phys. Chem. C.* **2016,** *120,* 9702 - 9712. https://doi.org/10.1021/acs.jpcc.6b03195
15. G.K Das, S. Anand, S. Acharya and R.P. Das. Preparation and decomposition of ammoniumjarosite at elevated temperatures in $H_2O(NH_4)_2SO_4H_2O$ media. *Hydrometallurgy*. **1995,** *38 (3),* 263-276. https://doi.org/10.1016/0304-386X(94)00064-A
16. C. Drouet and A. Navrotsky. Synthesis, characterisation and thermo-chemistry of K-Na-H_3O jarosites. *Geochim. Cosmochim. Acta,* **2003**, 67, 2063-2076. DOI: 10.1016/S0016-7037(02)01299-1
17. A. M. L. Smith, K. A. Hudson-Edwars, W.E. Dubbin, K. Wright. Dissolution of jarosite [$KFe_3(SO_4)_2(OH)_6$] at pH 2 and 8: Insights from batch experiments and computational modelling. *Geochem. Et Cosmochim. Acta.* **2006,** *70 (3),* 608-621.
18. C. Drouet, K. L. Pass, D. Baron, S. Draucker, A. Navrotsky. Thermochemistry of jarosite-alunite and natrojarosite-natroalunite solid solutions. *Geochim. Et Cossmochim. Acta.* **2004,** ***6.8 (10),*** 2197-2205. https://doi.org/10.1016/j.gca.2003.12.001
19. E. Salinas, E. Cerecedo, M. Ramírez, F. Patiño, M. Pérez. Kinetics ok alkaline decomposition and cyanidation of argentian rubidium jarosite in NaOH medium. *Metall. And Mater. Trans. B.* **2012,** *43B (5),* 1027-1033. https://doi.org/10.1007/s11663-012-9697-4
20. M. Perez-Labra, A. Romero-Serrano, E. Salinas-Rodriguez, E. O. Avila-Davila, M. Reyes-Perez. Synthesis, termo chemistry and kinetics of alkaline decomposition of rubidium jarosite in $Ca(OH)_2$ media. *Metall and Mater. Trans. B.* **2012,** *43 (4),* 773-780. https://doi.org/10.1007/s11663-011-9601-7
21. F. Patiño, I. A. Reyes, M. U. Flores, T. Pandiyan, A. Roca, M. Reyes, J. Hernández. Kinetic modeling and experimental design of the sodium aresenojarosite decomposition in alkaline media: Implications. *Hydrometallurgy*. **2013,** *137*, 115-125. https://doi.org/10.1016/j.hydromet.2013.05.005
22. F. Patiño, M.U. Flores, I.A. Reyes, H. Islas, M. Reyes and G. Juárez. Kinetic Modeling of the alkaline decomposition and cyanidation of Argentian plumbojarosite. *J. Mex. Chem. Soc.* **2014,** *58 (1),* 3-10. http://www.scielo.org.mx/pdf/jmcs/v58n1/v58n1a2.pdf
23. L. Gunneriusson, A. Sandström, A. Holmgren, E. Kuzmann, K. Kovacs, A. Vértes. Jarosite inclusion of fluoride and its potential significance to bioleaching of sulphide minerals. *Hydrometallurgy*. **2009,** *96 (1-2),* 108-116. https://doi.org/10.1016/j.hydromet.2008.08.012
24. W. Xu, Z. Xie, X. Cui, K. Zhao, L. Zhang, L. Mai and Y. Wang. Direct growth of an economic green energy storage material: Amonocrystalline jarosite-$KFe_3(SO_4)_2(OH)_6$ - nanoplates@rGO hybrid as a superior lithium-ion battery cathode. *J. Mater. Chem. A.* **2016**, *10,* 3735-3742. DOI: 10.1039/c5ta10622b
25. Y.L. Ding, Y. Wen, P.A. Van Aken, J. Maier, Y. Yu, Jarosite nanosheets fabricated via room-temperature synthesis as cathode materials for high-rate lithium ion batteries, *Chemistry of Materials*, **2015,** *27 (8),* 3143-3149. https://doi.org/10.1021/acs.chemmater.5b00849
26. T. Inami, M. Nishiyama, S. Maegawa and Y. Oka. Magnetic structure of the *kagomé* lattice antiferromagnet potassium jarosite $KFe_3(SO_4)_2(OH)_6$. *Phys. Rev. B: Condens. Matter Mater. Phys.* **2000,** *61,* 12181. DOI: https://doi.org/10.1103/PhysRevB.61.12181

27. L.C. Basciano and R.C. Peterson. Crystal chemistry of the natrojarosite-jarosite and natrojarosite-hydronium jarosite solid-solution series: A synthetic study with full Fe site occupancy. *Am. Mineral.*, **2008,** *93,* 853-862. https://doi.org/10.2138/am.2008.2731
28. H. Nagano and I. Taniguchi. Synthesis of $Li_2FeP_2O_7$/Carbon nanocomposite as cathode materials for Li-ion batteries. *J. Power Sources,* **2015,** *298,* 280-284. https://doi.org/10.1016/j.jpowsour.2015.08.068
29. W. Naiteng, T. Wendi, S. Jinke, Q. Xiaoguang, S. Tao, Z. Jianguo, L. Xianming and Z. Yun, Facile fabrication of a jarosite ultrathin $KFe_3(SO_4)_2(OH)_6$@rGO nanosheet hybrid composite with pseudocapacitive contribution as a robust anode for lithium-ion batteries, *Inorg. Chem. Front.* **2019,** *6,* 192-198. https://doi.org/10.1039/C8QI01165F
30. J. Qian, L. Lui, J. Yang, S. Li, X. Wang, H. Zhuang & Y. Lu, Electrochemical surface passivation of $LiCoO_2$ particles at ultrahigh voltage and its applications in lithium-based batteries, *Nat. Commu.*, **2018**, *9 (1),* 4918. https://doi.org/10.1038/s41467-018-07296-6
31. Y. Jiang, C. Qin, P. Yan and M. Sui. Origins of capacity and voltage fading of $LiCoO_2$ upon high voltage cycling, *J. Mater. Chem. A.*, **2019,** *7,* 20824-20831. https://doi.org/10.1039/C9TA06579B
32. P. Sandineni, H. Yaghoobnejad Asl, A. Choudhury. Kagomé lattices as cathode: Effect of particle size and fluoride substitution on electrochemical lithium insertion in sodium and ammonium jarosites, *Journal of Solid State Chemistry*, **2016**, *242,* 78-86. DOI: 10.1016/j.jssc.2016.02.022
33. J. E. Dutrizac and S. Kaiman. Synthesis and properties of jarosite type-compounds. *Can. Mineral.* **1976,** *14 (2)*, 151-158 (1976). https://pubs.geoscienceworld.org/canmin/article-abstract/14/2/151/11094/Synthesis-and-properties-of-jarosite-type?redirectedFrom=fulltext
34. J.W. Brown. A chemical study of some synthetic potassium-hydronium jarosites. *Can. Mineral.* **1970,** *10(4)*,696-703. https://pubs.geoscienceworld.org/canmin/article-abstract/10/4/696/10782/A-chemical-study-of-some-synthetic-potassium?redirectedFrom=fulltext
35. W. Kunda & H. Veltman. Decomposition of Jarosite. *Metall. Mater. Trans. B,* **1979,** *10,* 439-446. htpps://doi.org/10.1007/BF02652517
36. F. Patiño & J. Ramírez. Síntesis y caracterización de argentojarosita y plumbojarosita (In Spanish). *Rev. Soc. Quím. Mex.* **1993,** *37 (2),* 51-62.
37. J.E. Dutrizac and D.J. Hardy. The behaviour of thiocyanate and the cyanate during jarosite precipitation. *Hydrometallurgy,* **1997,** *45 (1-2),* 83-95. https://doi.org/10.1016/S0304-386X(96)00079-5
38. M. Cruells, A. Roca, F. Patiño, E. Salinas, I. Rivera. Cyanidation kinetics of argentian jarosite in alkaline media. *Hydrometallurgy*, ***2000,*** *55 (2),* 153-163. https://doi.org/10.1016/S0304-386X(99)00072-9
39. J.L. Cadena, J.M. Chimeros, I. Queralt, M. Viladevall, K. Flores y F. Pérez. Efecto del mineral de ganga en la síntesis de jarosita de potasio y su distribución de tamaños de partículas (In spanish). *Boletín de Mineralogía.* **2006,** *17 (1),* 21-28
40. A. Roca, F. Patiño, I. Rivera, L. Hernández, M. Pérez, E. Salinas and M. Reyes. Decomposition and Cyanidation Kinetics of the Argentian Ammonium Jarosite in NaOH Media. *J. Mex. Chem. Soc.,* **2007,** *51 (2),* 47-54. http://www.scielo.org.mx/pdf/jmcs/v51n2/v51n2a2.pdf